Structure and radiative transitions of the hydrogen atom moving in a strong magnetic field

1994 J. Phys. B: At. Mol. Opt. Phys. 27 1073

(http://iopscience.iop.org/0953-4075/27/6/008)

J. Phys. B: At. Mol. Opt. Phys. 27 (1994) 1073–1090. Printed in the UK

Structure and radiative transitions of the hydrogen atom moving in a strong magnetic field

A Y Potekhin[†]

Department of Theoretical Astrophysics, A F Ioffe Institute for Physics and Technology,
Politekhnicheskaya 26, St Petersburg, 194021, Russia
and
Nordita, Blegdamsvej 17, Copenhagen Ø, 2100, Denmark

Received 18 October 1993, in final form 23 December 1993

Abstract. The discrete spectrum of the hydrogen atom moving across a strong magnetic field ($B = 7 \times 10^{11}$–7×10^{12} G) is studied by expanding wavefunctions over a complete orthogonal basis, whose single term provides a correct description of an atomic state at large pseudomomenta K of the transverse motion. Wavefunctions, energies, atomic sizes and oscillator strengths of radiative transitions are calculated and analysed in a wide range of K values. All these quantities undergo radical changes when the atom moves across the field. The discrete spectrum remains infinite at arbitrary K, although the mean transverse velocity cannot exceed some maximum value for the bound states. Oscillator strengths change by orders of magnitude and some dipole selection rules are violated.

1. Introduction

Very strong magnetic fields $B \sim 10^{12}$ G are typical in the vicinity of neutron stars. A study of atoms in these huge fields is of theoretical interest as well as of great importance for the interpretation of astrophysical observations (Pavlov *et al* 1994). A neutron star accretes mostly hydrogen-rich interstellar matter. Therefore the simplest case of the hydrogen atom is also the most important one.

The relative strength of the Lorentz forces with respect to the Coulomb ones is usually measured by the parameter $\gamma = \hbar\omega_B/(2\ \mathrm{Ryd}) = B/(2.35 \times 10^9\ \mathrm{G})$, where $\omega_B = eB/(m_e c)$ is the electron cyclotron frequency, B is the magnetic field strength and $\mathrm{Ryd} = e^4 m_e/(2\hbar^2) = 13.6$ eV is the ionization potential of the field-free hydrogen atom. Many investigations have been devoted to the structure and radiative transitions of a hydrogen atom which is placed in a strong magnetic field ($\gamma \gtrsim 1$) but does not move across it. The Hamiltonian is axially symmetric in this case. In earlier studies (see, e.g., Garstang (1977) for a review), the adiabatic approximation was mostly employed. Simple variational ansatzes have also been used. In recent years a number of non-adiabatic studies have been carried out (Xi *et al* 1992, Wunner and Ruder 1987, and references therein). Oscillator strengths of the hydrogen atom in various magnetic fields have been calculated with high accuracy by Forster *et al* (1984).

The problem of an atom moving across a magnetic field is much more complicated, because it is essentially three dimensional. The first theoretical study of this problem was carried out by Gorkov and Dzyaloshinsky (1968) for an exiton. Avron *et al* (1978), Johnson

---

[†] E-mail: pav@astro.pti.spb.su

0953-4075/94/061073+18$19.50

et al (1983) and Baye and Vincke (1990) developed a general theoretical treatment of atoms and ions in magnetic fields. Burkova *et al* (1976) investigated so-called *decentred states* in the framework of the adiabatic approximation at very large pseudomomenta K of the motion across the field. In these states the electron is localized far from the nucleus. Baye *et al* (1992) obtained similar results using the multipole expansion of the Coulomb term in the Hamiltonian. Ipatova *et al* (1984) estimated the validity of the adiabatic approximation at high transverse pseudomomenta, and of the perturbation approach at low K. The perturbation approach was used by Vincke and Baye (1988) who calculated the energies of the four lowest states of a slowly moving hydrogen atom, and by Pavlov and Mészáros (1993) who considered various physical effects of atomic motion in the magnetic field. Finally, Vincke *et al* (1992) have calculated binding energies and wavefunctions of the hydrogen atom moving in strong magnetic fields with various transverse pseudomomenta. They used a non-orthogonal variational basis whose transverse part has been generated with the help of canonical transformations of the Hamiltonian.

The main aims of this paper are: (i) to present an alternative numerical technique based on an expansion of a wavefunction over some appropriate orthogonal basis which is more convenient in very strong magnetic fields; and (ii) to calculate the effects of transverse motion on atomic sizes and bound–bound oscillator strengths. In section 2 we recall the Hamiltonian and wavefunction transformations and describe the adiabatic, perturbation and multiconfiguration techniques which are used in further calculations. Numerical results are presented and discussed in section 3. Concluding remarks are given in section 4.

2. Basic equations

2.1. *Hamiltonian transformations*

The Hamiltonian of a hydrogen atom moving in a homogeneous magnetic field $\boldsymbol{B}$ (directed along the z-axis) is the sum of proton and electron kinetic terms and the Coulomb potential,

$$H = \pi_{\mathrm{p}}^2/(2m_{\mathrm{p}}) + \pi_{\mathrm{e}}^2/(2m_{\mathrm{e}}) + q_{\mathrm{e}}q_{\mathrm{p}}/|\boldsymbol{r}_{\mathrm{e}} - \boldsymbol{r}_{\mathrm{p}}| \tag{1}$$

where

$$\pi_i = m_i\dot{\boldsymbol{r}}_i = \boldsymbol{p}_i - \frac{q_i}{c}\boldsymbol{A}(\boldsymbol{r}_i) \tag{2}$$

is the kinetic momentum operator of the ith particle (Johnson and Lippmann 1949), the subscript i = e or i = p indicates electron or proton, respectively; $\boldsymbol{p}_i = -i\hbar\nabla_i$ is the canonical momentum, m_i is the mass, $q_{\mathrm{p}} = -q_{\mathrm{e}} = e$ is the charge, and $\boldsymbol{A}(\boldsymbol{r})$ is the vector potential of the field. The spin terms are omitted in (1) since we neglect relativistic effects and assume spin projections on the z-axis to be fixed. Components of the pseudomomentum

$$\boldsymbol{k}_i = \pi_i + \frac{q_i}{c}\boldsymbol{B} \times \boldsymbol{r}_i \tag{3}$$

are single-particle constants of motion. The total pseudomomentum $\boldsymbol{K} = \boldsymbol{k}_{\mathrm{e}} + \boldsymbol{k}_{\mathrm{p}}$ is the atomic constant of motion which generates velocity boosts (Johnson *et al* 1983). Thus it may be used to describe the general motion of the atom in a magnetic field. The components (K_x, K_y, K_z) commute with each other owing to the zero net charge of the atom. We shall consider states in which all the components have definite values. Eigenfunctions of $\boldsymbol{K}$ in the coordinate representation (Gorkov and Dzyaloshinsky 1968) are

$$\Psi(\boldsymbol{r}_e, \boldsymbol{r}_p) = \exp\left[\frac{i}{\hbar}\left(\boldsymbol{K} + \frac{e}{c}\boldsymbol{B} \times \boldsymbol{r}\right) \cdot \boldsymbol{R}\right] \psi(\boldsymbol{r}) \tag{4}$$

where $\boldsymbol{R} = (m_e/M)\boldsymbol{r}_p + (m_p/M)\boldsymbol{r}_e$ and $\boldsymbol{r} = \boldsymbol{r}_e - \boldsymbol{r}_p$ are the centre-of-mass and relative coordinates, and $M = m_e + m_p$ is the total mass. Henceforth we shall assume $K_z = 0$, since the motion of an atom as a whole along the magnetic field does not affect its internal structure, thus it is of minor physical interest. Besides, we shall choose the y-axis directed along $\boldsymbol{K}$.

The Hamiltonian (1) can be represented in the form

$$H = \Pi^2/(2M) + \pi^2/(2\mu) - e^2/r \tag{5}$$

where $\boldsymbol{\Pi} = M\dot{\boldsymbol{R}} = \boldsymbol{\pi}_e + \boldsymbol{\pi}_p$ and $\pi = \mu\dot{\boldsymbol{r}} = (m_p/M)\boldsymbol{\pi}_e - (m_e/M)\boldsymbol{\pi}_p$ are the collective and relative kinetic momenta, and $\mu = m_e m_p/M$ is the reduced mass.

When the atom moves, the field tends to draw the electron apart from the proton in the x-direction, breaking the axial symmetry. Therefore the most appropriate choice of a coordinate system and the gauge of the vector potential to treat the problem is no longer evident. It is convenient to define some basic electron–proton separation $\boldsymbol{r}_B$ in the xy plane and to regard the deviation from it, $\boldsymbol{r}' = \boldsymbol{r} - \boldsymbol{r}_B = (\boldsymbol{r}'_\perp, z)$, as an independent variable. It is also useful to consider the axial gauge $\boldsymbol{A}(\boldsymbol{r}) = \frac{1}{2}\boldsymbol{B} \times (\boldsymbol{r} - \boldsymbol{r}_A)$ centred at an arbitrary point $\boldsymbol{r}_A$ in the xy plane. Then, taking into account (4), one comes to the Hamiltonian of relative motion H_{rel}, which has been presented by Vincke *et al* (1992). The accompanying transformation of the wavefunction includes the space shift to $\boldsymbol{r}_B$ and the phase transformation (Landau and Lifshitz 1976) related to the gauge parameter $\boldsymbol{r}_A$.

The general form of H_{rel} contains terms which couple collective and relative canonical variables. Some of these terms are proportional to μ^{-1} and may lead to a strong perturbation, significantly complicating numerical treatment. To avoid this complication, the condition

$$\boldsymbol{r}_A = [(m_p - m_e)/M]\boldsymbol{r}_B \tag{6}$$

should be imposed. Under this condition one obtains the set of Hamiltonians, depending on two real parameters (r_{Bx}, r_{By}), which has been used by Vincke *et al* (1992) to generate the variational basis of their calculations:

$$H_{\mathrm{rel}} = K_z^2/(2M) + p_z^2/(2\mu) + H_\perp - e^2/|\boldsymbol{r}_B + \boldsymbol{r}'|. \tag{7}$$

The transverse kinetic part $H_\perp$ may be written as

$$H_\perp = (\pi')^2/(2\mu) - \frac{e}{m_p c}\boldsymbol{B} \cdot (\boldsymbol{r}' \times \boldsymbol{p}) + H_K \tag{8}$$

where

$$\pi' = \boldsymbol{p}_\perp + \frac{e}{2c}\boldsymbol{B} \times \boldsymbol{r}' \tag{9}$$

$$H_K = \frac{(K')^2}{2M} + \frac{e}{Mc}\boldsymbol{K}' \cdot (\boldsymbol{B} \times \boldsymbol{r}') \tag{10}$$

$$\boldsymbol{K}' = \boldsymbol{K} + \frac{e}{c}\boldsymbol{B} \times \boldsymbol{r}_B. \tag{11}$$

Note that π' coincides with $\pi_{e\perp}$ except for the argument change.

The term H_K can be eliminated by the choice $r_B = r_C$, where

$$r_C = \frac{c}{eB^2} B \times K \tag{12}$$

is the relative guiding centre. Then $K' = 0$, and one comes to the 'shifted' Hamiltonian (7), (8) with $H_K = 0$, exploited by Gorkov and Dzyaloshinsky (1968), Burkova *et al* (1976), Herold *et al* (1981) and Ipatova *et al* (1984). The conventional choice $r_B = 0$, in contrast, keeps H_K non-zero (with $K' = K$) but makes the potential in (7) symmetric.

2.2. *Basis set of wavefunctions*

The transverse part of a wavefunction of an isolated electron with a definite z-projection $m\hbar$ of the angular momentum in a magnetic field is a Landau function (Landau and Lifshitz 1976)

$$\Phi_{Nm}(r_{e\perp}) = (2\pi)^{-1/2} \exp(\mathrm{i}m\varphi) a_M^{-1} I_{N-m,N}(\rho^2/2a_M^2) \tag{13}$$

where ρ and φ are the polar coordinates of $r_{e\perp}$ in the xy plane, $I_{NN'}(\xi)$ is the Laguerre function (Sokolov and Ternov 1968), $N = 0, 1, 2, \ldots$ is the number of the Landau level ($m = N, N-1, \ldots$), and $a_M = (\hbar c/eB)^{1/2}$ is the magnetic length. Functions (13) solve the Schrödinger equation with a single-particle transverse Hamiltonian $\pi_{e\perp}^2/(2m_e)$, where π_e is defined by equation (2) with $A(r) = \frac{1}{2} B \times r$. From equation (8) the remarkable fact that functions (13) with $r'_\perp$ substituted for $r_{e\perp}$ are also the eigenfunctions of $H_\perp$ without H_K follows. The quantum numbers N and $\widetilde{N} = N - m$ are then the Landau numbers of the electron and the proton in the absence of the Coulomb interaction, corresponding to the transverse energy

$$E_{Nm}^\perp = \frac{m_e}{\mu}(N + \tfrac{1}{2})\hbar\omega_B - \frac{m_e}{m_p} m\hbar\omega_B = \left[N + \tfrac{1}{2} + \frac{m_e}{m_p}(\widetilde{N} + \tfrac{1}{2})\right]\hbar\omega_B. \tag{14}$$

The *continuum boundary* is $E_{00}^\perp = \hbar\omega_B(1 + m_e/m_p)/2$.

A wavefunction $\psi_\kappa(r')$, which solves the equation

$$H_{rel}\psi_\kappa = E_\kappa \psi_\kappa \tag{15}$$

may be expanded over the complete set of the Landau functions in the xy plane:

$$\psi_\kappa(r') = \sum_{N'm'} \Phi_{N'm'}(r'_\perp) g_{N'm';\kappa}(z). \tag{16}$$

This expansion is most convenient, if $\gamma \gtrsim 1$. Then, if the influence of H_K is not too great, one can select a leading (Nm) term and ascribe to the atomic state three numbers $\kappa = (N, m, \nu)$, where $\nu = 0, 1, 2, \ldots$ consequently numerates longitudinal energy levels

$$E_{Nm\nu}^\parallel = E_{Nm\nu} - E_{Nm}^\perp \tag{17}$$

starting from the deepest one. The z-parity of the wavefunction is $(-1)^\nu$. Since the energy distances between $E_{Nm}^\perp$ grow with γ, all the levels become metastable at $\gamma \gg 1$, except for those with $N = 0$ and small $(-m)$.

Substituting (16) into (15), multiplying by $\Phi_{N''m''}(\boldsymbol{r}'_\perp)$ and integrating over $\boldsymbol{r}'_\perp$, one arrives at the set of coupled equations

$$\left[-\frac{\hbar^2}{2\mu}\frac{\mathrm{d}^2}{\mathrm{d}z^2} + V_{N''m'',N''m''}(z) + \langle N''m''|H_K|N''m''\rangle + E^{\perp}_{N''m''} - E^{\perp}_{Nm} - E^{\parallel}_{Nm\nu}\right] g_{N''m'';Nm\nu}(z)$$

$$= -\sum{}' \left(V_{N''m'',N'm'}(z) + \langle N''m''|H_K|N'm'\rangle\right) g_{N'm';Nm\nu}(z) \qquad (18)$$

where summing is over all the pairs (N', m') except for (N'', m''), and

$$V_{N''m'',N'm'}(z) = \left(N''m''\right| -e^2/|\boldsymbol{r}_\mathrm{B} + \boldsymbol{r}'| \left|N'm'\right)_\perp \qquad (19)$$

is the effective potential discussed in the appendix.

The *infinite* system (18) is equivalent to the Schrödinger equation (15). Truncating the sum (16), one comes to the *finite* system, which solves (15) approximately. Such a solution is consistent with the variational principle on the truncated basis.

The potentials $V_{N''m'',N'm'}(z)$ with $m'' \neq m'$ are equal to zero if $\boldsymbol{r}_\mathrm{B} = 0$, whereas the terms $\langle N''m''|H_K|N'm'\rangle$ vanish at $\boldsymbol{r}_\mathrm{B} = \boldsymbol{r}_\mathrm{C}$. Thus for an atom at rest ($r_\mathrm{C} = 0$) the summing over m' drops out, and the system (18) splits into disconnected subsystems corresponding to separate values of m, which becomes a good quantum number. This particular case has been investigated by many authors (e.g. Wunner and Ruder (1987), and references therein). In section 3 we shall solve system (18) in the general case of a moving atom.

2.3. *Adiabatic approximation*

At $\gamma \gg 1$ the leading term in (16) may become large compared with side terms. Then the *adiabatic approximation* may be applied:

$$\psi_{Nm\nu}(\boldsymbol{r}') \approx \psi^{\mathrm{ad}}_{Nm\nu}(\boldsymbol{r}') \equiv \Phi_{Nm}(\boldsymbol{r}'_\perp) g^{\mathrm{ad}}_{Nm\nu}(z) \qquad (20)$$

and (18) acquires the form of a one-dimensional Schrödinger equation with the potential $V_{Nm}(z) \equiv V_{Nm,Nm}(z)$. The number ν counts the nodes of $g^{\mathrm{ad}}_{Nm\nu}(z)$. The validity of this approximation depends significantly on the parameter $\boldsymbol{r}_\mathrm{B}$ used. Ipatova *et al* (1984) have shown that for the *ground* state the perturbation theory based on the conventional choice $\boldsymbol{r}_\mathrm{B} = 0$ is valid for small K, whereas for large K the choice $\boldsymbol{r}_\mathrm{B} = \boldsymbol{r}_\mathrm{C}$ is appropriate. The latter conclusion is also valid for excited states since the non-diagonal effective potentials $V_{N''m'',N'm'}(z)$ (unlike $\langle N''m''|H_K|N'm'\rangle$) vanish at $r_\mathrm{B} \to \infty$ (see the appendix).

Generally, one may always choose $r_\mathrm{B} \leqslant r_\mathrm{C}$. When an atom moves so that $r_\mathrm{C} \ll a_\mathrm{M}$, the effective potential $V_{Nm}(z)$ deviates from the one-dimensional Coulomb potential only near the origin. In this case the energies $E^{\parallel}_{Nm\nu}$ at $\gamma \gg 1$ are described by the Rydberg series with the effective quantum numbers $[\nu/2 + O(\ln\gamma)^{-1}]$ for $\nu = 0, 2, 4, \ldots$ and $[(\nu+1)/2 + O(\gamma^{-1})]$ for $\nu = 1, 3, 5, \ldots$ (Hasegawa and Howard 1961, Haines and Roberts 1969). The transverse atomic size is $l_\perp \sim a_\mathrm{M} \ll a_\mathrm{B}$ (equation (24)), where $a_\mathrm{B} = \hbar^2/(m_\mathrm{e}e^2)$ is the Bohr radius, whereas the longitudinal size is determined by the binding energy,

$$l_z \sim 0.5\hbar(m_\mathrm{e}|E^{\parallel}|)^{-1/2} \quad \text{if } \nu = 0 \qquad l_z \sim 0.8e^2/|E^{\parallel}| \quad \text{if } \nu = 1, 2, 3, \ldots. \qquad (21)$$

In the opposite case $r_\mathrm{C} \gg a_\mathrm{M}$, if $\boldsymbol{r}_\mathrm{B} = \boldsymbol{r}_\mathrm{C}$, one has $V_{Nm}(z) \approx -e^2/\sqrt{r_\mathrm{C}^2 + z^2}$. In the limiting case $r_\mathrm{C}/a_\mathrm{B} = Ka_\mathrm{B}/(\gamma\hbar) \gg 1$, low-lying states are determined by the oscillator-like part of this potential at $|z| \ll r_\mathrm{C}$ (Burkova *et al* 1976). Then the energies are

$$E^{\parallel}_{Nm\nu} = \frac{e^2}{r_\mathrm{C}}\left(-1 + \sqrt{a_\mathrm{B}/r_\mathrm{C}}(\nu + \tfrac{1}{2})\right) \qquad (22)$$

and the root-mean-square (RMS) atomic z-size $l_z = \langle N m \nu | z^2 | N m \nu \rangle^{1/2}$ grows as

$$l_z = (\nu + \tfrac{1}{2})^{1/2} (r_C^3 a_B)^{1/4} \propto (K/\gamma)^{3/4}. \tag{23}$$

This approximation is valid under the condition $l_z \ll r_C$, which requires $\nu \ll \sqrt{r_C/a_B}$. Higher levels are again driven by the Coulomb tails. Therefore the number of levels remains infinite, regardless of K and γ values. The levels with $N \geqslant 1$ or $m \leqslant -1$ are involved in the continuum at high γ or K, but all (00ν) levels lie below $E_{00}^{\perp}$, thus being really bound.

Transverse RMS sizes of the $\boldsymbol{r}'$-coordinate distribution equal

$$l_y = l_x' = a_M \sqrt{2N - m + 1}. \tag{24}$$

However, the electron density is shifted apart from the proton, so that the atomic x-size $l_x = \langle (x_e - x_p)^2 \rangle^{1/2}$ becomes $l_x = \sqrt{l_x'^2 + r_C^2}$. Owing to the large atomic sizes and small binding energies at large r_C, atoms are easily destroyed by collisions. Therefore the decentred states can be observed either at very low densities or at very strong fields ($\gamma \gg 1$).

2.4. *Perturbation approach*

Let us consider the Hamiltonian (7) with $r_B = 0$. When K is small, one may treat H_K as a perturbation, starting from the wavefunctions and energies of the fixed atom. This approach gives

$$E_\kappa(K) = E_\kappa(0) + K^2/(2M_\kappa^\perp) \tag{25}$$

where the effective transverse mass $M_\kappa^\perp$ depends on the field strength.

Since the second-order perturbation cannot raise the ground level (Landau and Lifshitz 1976), it is evident that $M^\perp > M$ for the ground state. In fact, $M^\perp$ is even much greater for excited states, since the magnetic field hampers the transverse motion of loosely bound charges.

Vincke and Baye (1988) used a variational method for the zero-order computations. Alternatively, starting from the adiabatic solution for the fixed atom, one can easily express $M_{Nm\nu}^\perp$ in terms of the longitudinal overlap integrals $\langle g_{Nm\nu}^{\mathrm{ad}} | g_{N'm'\nu'}^{\mathrm{ad}} \rangle_\parallel$ and binding energies $|E_{N'm'\nu'}^{\parallel(\mathrm{ad})}(K = 0)|$, where $N' = N \pm 1$, $m' = m \pm 1$, $\nu' = \nu$, $\nu \pm 2$, $\nu \pm 4, \ldots$ are the quantum numbers of levels admixed by the perturbation (with the common restrictions $N' \geqslant 0$, $m' \leqslant N'$, $\nu' \geqslant 0$). For states with $N = 0$ this has been done by Pavlov and Mészáros (1993) who investigated kinematic, thermodynamic and spectroscopic effects of the motion of the hydrogen atom in strong magnetic fields. According to their estimates, limitations on the validity ranges of the perturbation approach are rather strong, especially for the hydrogen-like levels.

2.5. *Multiconfiguration approach*

Various methods have been applied to solving the set of equations (18) in the particular case of an atom at rest, when the double sum in (18) reduces to the single one. Simola and Virtamo (1978) developed a finite-difference iterative scheme, treating 'side' equations separately from the leading one. Friedrich (1982) used a variational expansion of $g_{N'm;\kappa}(z)$, which led to a matrix eigenvalue problem. Wunner and Ruder (1982) and Rösner *et al*

(1984) adjusted the multiconfiguration Hartree–Fock (MCHF) method to this case (Froese Fischer 1977).

We have employed an MCHF-like scheme for finding E_κ and $g_{N'm'\nu';\kappa}(z)$ from (18) in the general case of the moving atom. For each given state $\kappa = |Nm\nu\rangle$, an initial approximation of the leading term was the adiabatic solution obtained in a way similar to the previously described one (Potekhin and Pavlov 1993). Then a nested iterative procedure started. At each nth inner iteration: (i) the system (18) was solved with the results of the preceding iteration $g^{(n-1)}_{N'm'}(z)$ substituted into the right-hand-side sum; (ii) thus obtained longitudinal functions $\tilde{g}^{(n)}_{N'm'}(z)$ were normalized so that $\int |\tilde{g}^{(n)}_{N'm'}(z)|^2\,\mathrm{d}z = 1$; and (iii) the matrix eigenvalue problem

$$\sum_{N'm'} \langle \tilde{g}_{N''m''} | [-\hbar^2/(2\mu)\,\mathrm{d}^2/\mathrm{d}z^2 + E^{\perp}_{N''m''}]\delta_{N''N'}\delta_{m''m'} \\ + V_{N''m'';N'm'}(z) + \langle N''m''|H_K|N'm'\rangle\, |\tilde{g}_{N'm'}\rangle_{\|} c_{N'm'} = E c_{N''m''} \qquad (26)$$

was solved by the inverse iteration (Parlett 1980) with the shift $E^{(n-1)}$, using the LU factorization code of Fletcher (1988). As a result, the next (nth) approximation $g^{(n)}_{N'm'}(z) = c^{(n)}_{N'm'}\tilde{g}^{(n)}_{N'm'}(z)$ and $E^{(n)}$ was obtained. At the outer iteration, one more Landau orbital was included, and the procedure repeated. The process was terminated when a convergence of both energy value E and coefficients $c_{N'm'}$ was achieved. Once a solution at some γ, K and r_B is obtained, it may be used as the starting approximation at a slightly different value of one of these parameters. Then the outer iteration is no longer necessary.

In actual calculations we used the decentring parameter $r_\mathrm{B} = \eta r_\mathrm{C}$, $0 \leqslant \eta \leqslant 1$. Up to 32 Landau orbitals were included in the expansion (16). The longitudinal equations (21) have been solved using the combined shooting-direct method (Froese Fischer 1977). The longitudinal mesh consisted of up to 10 uniform pieces, which counted equal (from 20 to 80) number of points, the step h being doubled at the start of the next piece. The initial step $h = a_\mathrm{M}/20$ at $z = 0$ ensured an accuracy level better than 10^{-3} Ryd in energy and, typically, about 1% in oscillator strengths.

3. Results and discussion

3.1. Wavefunctions

Wavefunctions of the moving atom can most easily be found in the limits of low and high transverse pseudomomenta. In the first case ($r_\mathrm{B} \leqslant r_\mathrm{C} \to 0$) the effective potentials with $m' \neq m$ vanish, while the terms with $N' \neq N$ become small at $\gamma \gg 1$ due to the large energy differences $|E^{\perp}_{N'm} - E^{\perp}_{Nm}|$. In the opposite case $K \to \infty$ the representation 'with full shift' $r_\mathrm{B} = r_\mathrm{C}$ is appropriate, at which the non-diagonal effective potentials $V_{Nm,N'm'}(z)$ decrease rapidly regardless of field strength. Therefore in both limits a small number of terms may be kept in (16). For low-lying tightly bound states some intermediate (*mixing*) range of K exists, in which many Landau orbitals are coupled together, so that a way to select a leading term of the expansion becomes unclear. However, at $\gamma \gtrsim 300$ all energy levels can be traced diabatically either to low or to high K without any uncertainty, so that the numbering $|\kappa\rangle = |Nm\nu\rangle$ remains unambiguous in the mixing range.

The position of the critical K value around which the mixing takes place can be roughly estimated as $K_\mathrm{c} = \sqrt{2M|E^{\|}|}$. At $K > K_\mathrm{c}$ only the choice $\eta = 1$ remains practical for the treatment of the system (18), while choices $\eta \neq 1$ lead to divergence.

The expansion coefficients $c_{N'm'}$ with $N' \geqslant 1$ remain very small, reaching the maximum value for the ground state at $K = 0$. Thus the approximation assuming $N' = 0$ in (16) is justified for a moving atom not worse than for an atom at rest. For all hydrogen-like states (unlike tightly bound ones) a few terms of the expansion with $\eta = 1$ are sufficient at arbitrary K.

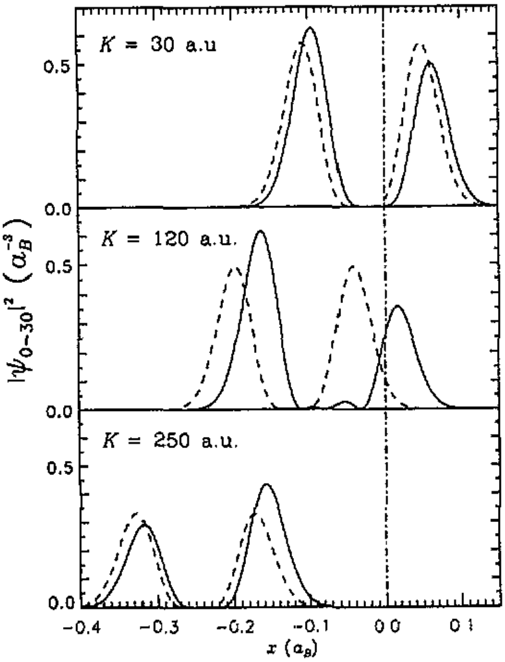

Figure 1. Square modulus of the wavefunction of the state $|0-30\rangle$ (full curves) compared with the adiabatic approximation (broken curves) in the full-shift representation at $B = 2.35 \times 10^{12}$ G.

Figure 1 shows the relative electron–proton probability density at $y = z = 0$ for $\gamma = 1000$, compared with the adiabatic results with $\eta = 1$. The shape of this function is asymmetric. At low K, when the decentring is small, its left side is higher because of the electric field induced in the comoving reference frame. At high K, in contrast, the whole function is leftward shifted, its right side being increased by the Coulomb attraction. In the mixing range additional details arise from the influence of neighbouring orbitals admixed. Nevertheless the adiabatic approximation gives a qualitatively correct impression of the real shape of the wavefunction.

The mean electron–proton separation is generally less than r_C. It depends on K, as shown in figure 2. These dependences are similar to those of 'optimal decentring' obtained by Vincke *et al* (1992) with the use of the adiabatic approximation. However, the quantity presented here has the clearer quantum-mechanical meaning of the average dipole moment divided by er_C. We see that at small K this quantity is relatively small for the lowest states, while at large K all the curves approach unity. In the intermediate range the dependences for the excited tightly bound states reveal non-monotonic features due to the approximate admixing of neighbouring states. A decrease in the field strength leads to sharper features and to more abrupt ground-state decentring.

Figure 3 presents the K dependences of the longitudinal atomic size l_z at $\gamma = 1000$ compared with the approximations (21) and (23). In agreement with the discussion in section 2.3, the former approximation is relatively good at small K, whereas the latter one works at $K \gg \gamma v^2 \hbar / a_B$.

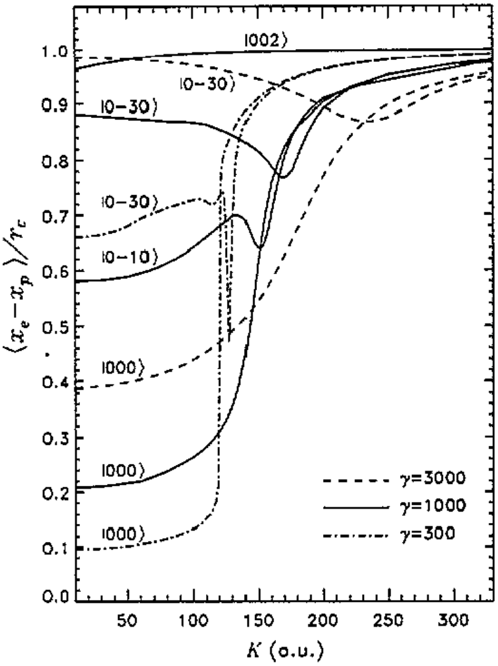

Figure 2. Ratio of the mean electron–proton separation to the relative guiding centre distance against transverse pseudomomentum K at $B = 7.05 \times 10^{12}$ G, 2.35×10^{12} G, and 7.05×10^{11} G.

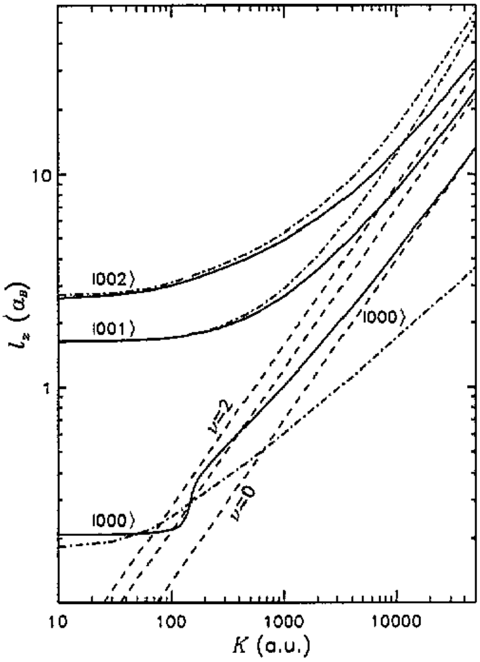

Figure 3. Longitudinal atomic sizes $l_z = \langle z^2 \rangle^{1/2}$ (full curves) compared with the approximations (21) (chain curves) and (23) (broken lines) at $B = 2.35 \times 10^{12}$ G.

3.2. Energy levels

When a free atom moves, the total momentum conservation results in its stability regardless of the total energy increase. For the motion across a magnetic field, the conserving quantity is the pseudomomentum $\boldsymbol{K}$, to which all values of the common continuum level $E^{\perp}_{00}$

correspond. Hence all states with total energies above $E_{00}^{\perp}$ are metastable. Their accurate treatment would include a simultaneous calculation of the open-channel (with $E_{N'm'}^{\perp} < E_{\kappa}$) and closed-channel ($E_{N'm'}^{\perp} > E_{\kappa}$) terms in (16), (18). However, since the admixture of the former terms is relatively small, one may exclude them from (16) and treat these states as quasibound ones. Thus the discrete spectrum can be extended above the continuum boundary $E_{00}^{\perp}$, as is illustrated in figure 4. At each K value a larger number of tightly bound states become really bound with the decrease in field strength.

Since $|E_{Nm\nu}^{\parallel}|$ decrease monotonically with increasing K, the tightly bound levels $(Nm0)$ cross hydrogen-like ones $(Nm'\nu)$, if $m' > m$. The exact crossings with the odd states cause no problems, since corresponding wavefunctions have different z-parities. In contrast to this, close to the anticrossing points with the even states one should exclude the orbitals $\Phi_{Nm'}$ and Φ_{Nm} from the expansions (16) for the states $|Nm0\rangle$ and $|Nm'\nu\rangle$, respectively, in order to avoid a numerical instability. Generally this reduction may lead to non-zero matrix elements $\langle Nm0|Nm'\nu\rangle$ and $\langle Nm0|H_{\text{rel}}|Nm'\nu\rangle$, calculated with the solutions on the reduced bases. Therefore an approach similar to perturbation theory for degenerate states may be applied to resolve the approximate crossings. In most cases the above-mentioned matrix elements became zero within our numerical accuracy. At $\gamma = 1000$ we have proved numerically that $|0m0\rangle/|00\nu\rangle$ energy gaps do not exceed 2×10^{-4} Ryd. The only exception *is the* $|002\rangle/|0-10\rangle$ *anticrossing with the binding energy* $E = 0.31$ *Ryd at* $K = 950$ *au*, for which the gap between the lower and upper E against K curves reaches ~ 0.005 Ryd in the E-direction compared with ~ 15 au in the K-direction, whereas for the $|002\rangle/|0-20\rangle$ anticrossing ($K = 452.8$ au, $E = 0.3807$ Ryd) the gap is as small as 10^{-4} Ryd compared with 0.1 au, respectively. Except for these narrow gaps, the diabatic curves are traced from low to high K without uncertainties.

A qualitatively new feature which appears at lower field strength (figures 4(*c*) and (*d*)) *is that some hydrogen-like levels with* $m \neq 0$ *become really bound at low* K. *This results in* anticrossings between hydrogen-like levels belonging to different m-manifolds. At $\gamma = 300$ these anticrossings are very narrow. The exception is $|0-12\rangle/|004\rangle$, which reveals the energy gap between $E = 0.160$ Ryd to $E = 0.182$ Ryd at $K = 33$ au. By a further increase in K, the wavefunction of the state with the higher binding energy (initially $|0-12\rangle$) acquires the properties of $|004\rangle$ (larger longitudinal size and more nodes), and *vice versa*.

The expectation value of the velocity of the transverse motion $\langle V\rangle = \partial E/\partial K$ is equal to $K/M^{\perp}$ at small K, but decreases as $e^3 B/(cK^2)$ at large K. For each state some maximum velocity is reached when the second derivative $\partial^2 E/\partial K^2$ turns to zero.

In figure 5(*a*) the numerically obtained energies are compared with the ($\eta = 1$)-adiabatic and perturbational ones. In agreement with the discussion in sections 2.3 and 2.4, the adiabatic curves rapidly approach the exact ones at K above the mixing range, where the perturbation method fails. The humps at the adiabatic curves at low K correspond to the behaviour (A11) of the effective potentials, which grow with r_{B}, if $r_{\text{B}} \ll 1$ and $m \neq 0$. In figure 5(*b*) the energies of the band $m = 0$ are compared with the harmonic approximation (22).

The discrete spectrum is infinite at each K value. This is proved by the fact that the number of states is infinite in the adiabatic approximation (section 2.3), which may be regarded as a variational ansatz. Since the adiabatic wavefunctions with the same (N, m) and different ν are orthogonal to each other, and since the number of bound states obtained variationally under the orthogonality condition cannot be greater than the number of true bound states, we may conclude that the latter number is actually infinite for the moving hydrogen atom. The opposite conclusion has been inferred by Baye *et al* (1992) from the parabolic approximation of the potential at large K. However, we have seen in section 2.3

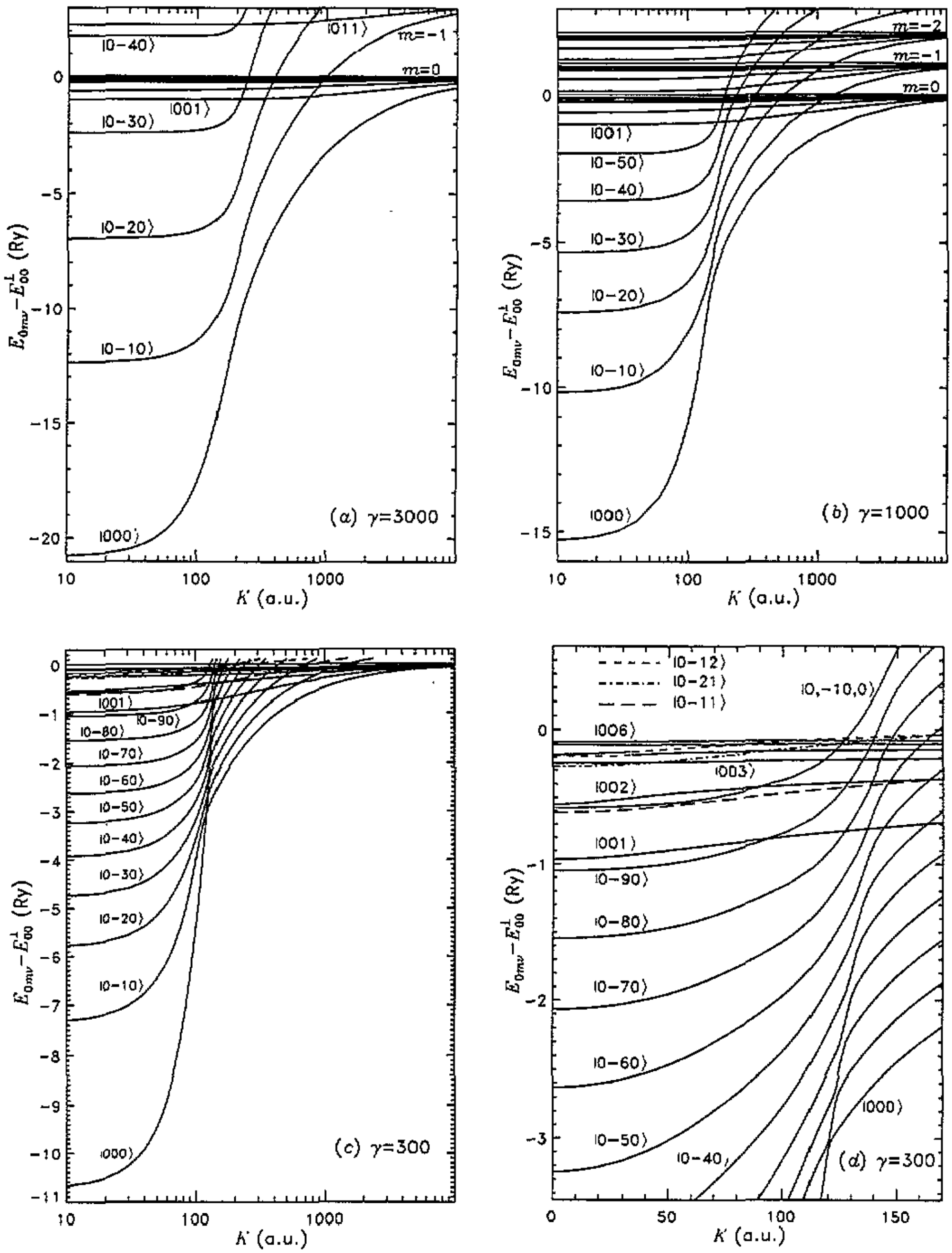

Figure 4. Energy spectrum against transverse pseudomomentum K at $B = 7.05 \times 10^{12}$ G (*a*), 2.35×10^{12} G (*b*), and 7.05×10^{11} G (*c*), (*d*).

that this approximation fails if ν is not small enough. Figure 5(*b*) confirms that the harmonic energies approach the exact ones at much higher K for higher ν values.

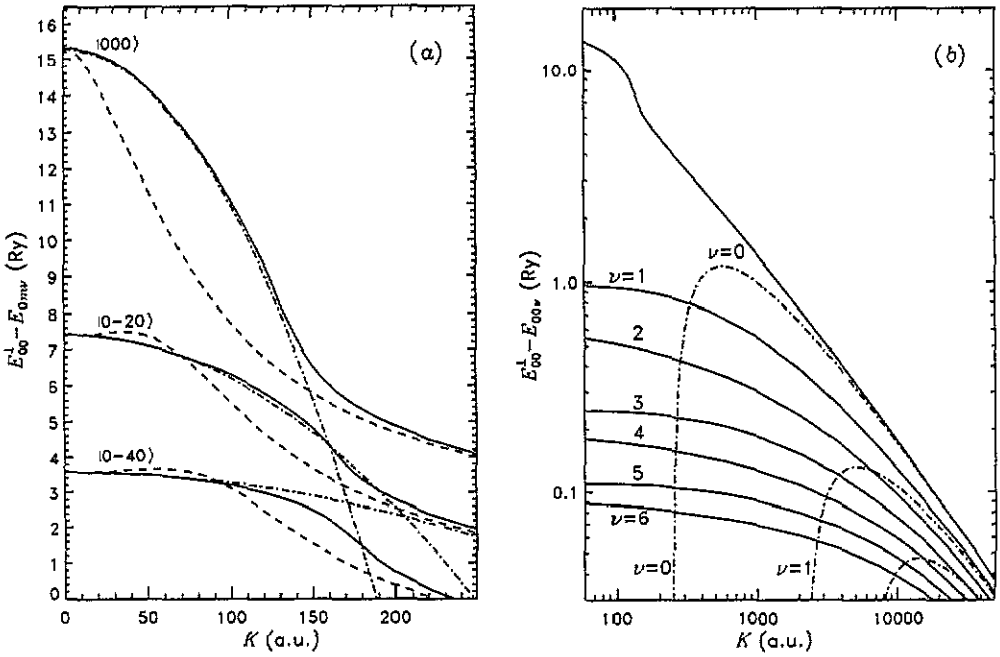

Figure 5. Comparison of exact binding energies (full curves) (*a*) with the second-order perturbation approximation (25) (chain curves) and the full-shift adiabatic approximation (broken curves), and (*b*) with the oscillator-like approximation (22) (chain curves) at $B = 2.35 \times 10^{12}$ G.

3.3. Radiative transitions

Having obtained wavefunctions and energies of initial $|i\rangle$ and final $|f\rangle$ bound states, one can calculate oscillator strengths of radiative transitions

$$f_{fi,\alpha} = \frac{\hbar\omega}{\mathrm{Ryd}} |D_{fi,-\alpha}/a_{\mathrm{B}}|^2 \tag{27}$$

where ω is the circular frequency, $\alpha = 0, \pm 1$ is the polarization index of incident radiation, corresponding to the polarization orts $e_0 = e_z$, $e_{\pm 1} = (e_x \pm \mathrm{i} e_y)/\sqrt{2}$, and $D_{fi,-\alpha}$ is the cyclic component of the dipole matrix element, which can be calculated either in the 'coordinate form'

$$\boldsymbol{D}^{(r)}_{fi} = \langle f|\boldsymbol{r}|i\rangle \tag{28}$$

or in the 'velocity form'

$$\boldsymbol{D}^{(\pi)}_{fi} = (\mathrm{i}\omega)^{-1}\langle f|\boldsymbol{\pi}|i\rangle . \tag{29}$$

Using the expansion (16) for the states $|i\rangle$ and $|f\rangle$, these matrix elements can be reduced to sums of one-dimensional (longitudinal) quadratures.

In fact we employed both forms, and used the concordance between them as one of the tests for calculation accuracy. For an atom at rest it has already been argued that the 'coordinate form' (28) is more relevant at $\gamma \gg 1$ for circular polarization (Potekhin and Pavlov 1993). For the moving atom this conclusion has been confirmed by the present

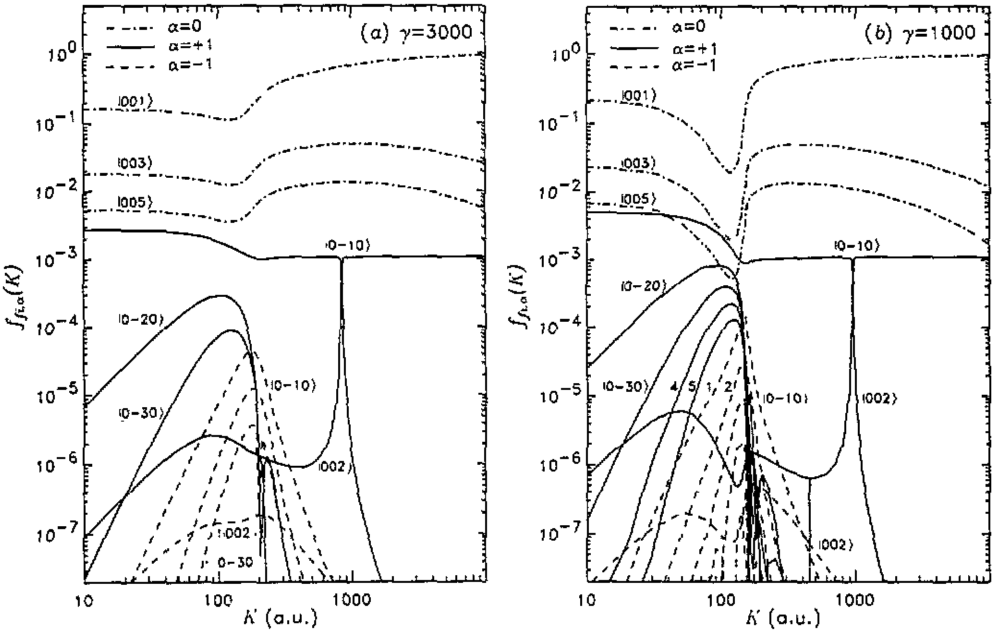

Figure 6. Oscillator strengths of radiative transitions from the ground state to the states marked near the lines at $B = 7.05 \times 10^{12}$ G (*a*) and 2.35×10^{12} G (*b*) for right circular (full curves), left circular (broken curves), and longitudinal (chain curves) polarization.

calculations, which required a significantly greater number of basis functions related to $N' > 0$ to be included in the expansion (16) for the numerical convergence of the matrix element (29), whereas a small number of such terms was enough for $D_{fi}^{(r)}$ convergence.

In contrast to the case of a field-free atom, the oscillator strengths of an atom in a magnetic field do depend on its motion. Figure 6 presents such dependences for the radiative transitions from the ground state $|000\rangle$ to some excited states marked near the curves. Because of the definite z-parity of each wavefunction, dipole transitions to the odd states are allowed only with the longitudinal polarization ($\alpha = 0$). Transitions to the even states $|0m0\rangle$ and $|002\rangle$ are allowed either with right ($\alpha = +1$) or with left ($\alpha = -1$) circular polarization. For a fixed atom ($K = 0$) an additional selection rule, $m_i - m_f = \alpha$, results from the angular momentum conservation. In particular, transitions from the ground state under the effect of the left-polarized radiation $\alpha = -1$ are possible only if the final state belongs to the continuum, since all states with $m > 0$ are involved in the continuum at $\gamma \gtrsim 0.15$ (see Rösner *et al* 1984). This selection rule is broken by the motion.

The strong resonance of the transition to $|002\rangle$ with $\alpha = +1$ is caused by the anticrossing with the state $|0-10\rangle$. Similarly, sharp dips on the $|0m0\rangle$ curves are due to anticrossings of these tightly bound states with hydrogen-like levels.

At lower field strengths the variations in the oscillator strengths with varying K become more prominent, as figure 7 demonstrates for $\gamma = 300$. Resonances at longitudinal polarization appear, caused by hydrogen-like level anticrossings discussed in section 3.2. Another unusual feature is that near $K \sim 100$ au the absorption of right-polarized radiation becomes stronger than that of longitudinally-polarized one.

Oscillator strength limits of the allowed transitions at $K \to 0$ in figures 6 and 7 correspond to the values presented by Forster *et al* (1984). Limits at large K can be found

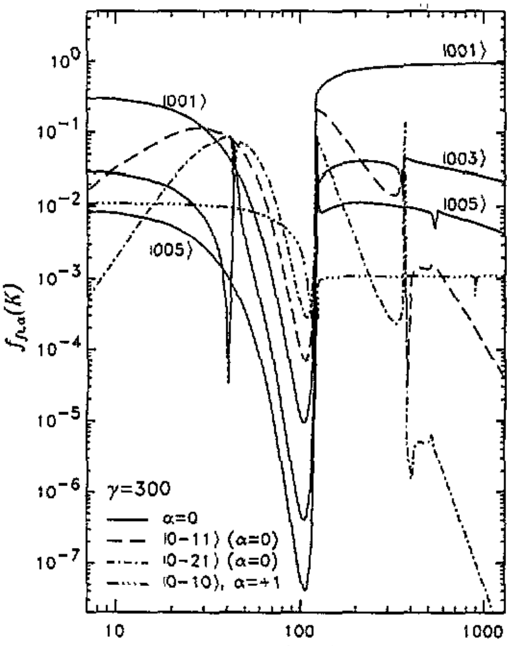

Figure 7. Oscillator strengths of radiative transitions from the ground state to odd hydrogen-like states at $B = 7.05 \times 10^{11}$ G for longitudinal polarization, compared with the transition to $|0-10\rangle$ for right circular polarization.

from the adiabatic approximation, which provides the explicit form of the transverse matrix elements (Potekhin and Pavlov 1993). Since effective potentials $V_{0m}(z)$ tend to each other at $K \to \infty$, the longitudinal matrix elements approach $\delta_{\nu_f\nu_i}$ for the circular polarization. This gives

$$f_{fi,+1} \simeq 2m_f\delta_{|m_f|,|m_i|+1}\delta_{\nu_f\nu_i}(m_e/m_p) \tag{30}$$

at $K \gg K_c$. To find longitudinal matrix elements for $\alpha = 0$, one may employ the oscillator-like approximation (section 2.3). Then one obtains

$$f_{fi,0} \simeq \nu_f\delta_{m_f m_i}\delta_{\nu_f,\nu_i+1} \tag{31}$$

at $K \gg \gamma\nu_f^2\hbar/a_B$. The calculated oscillator strengths in figures 6 and 7 behave in accordance with these estimates.

4. Conclusions

The expansion of wavefunctions over the complete orthogonal basis of the Landau states $|Nm\rangle$ is the conventional tool for studying atoms at rest in strong magnetic fields ($\gamma = B/(2.35 \times 10^9\ \mathrm{G}) \gtrsim 1$). In the present paper we have shown that an analogous expansion (16) remains convenient for hydrogen atoms moving in the field $\gamma \gg 1$. The advantage of this expansion is that the non-diagonal effective potentials vanish for both small *and large* transverse pseudomomenta K, if the shift parameter $r_B = r_C$ is used. Therefore the leading expansion term has the correct asymptotic properties. Besides, the orthogonality of the basis simplifies calculations of the matrix elements. A small number of terms provide satisfactory accuracy in the cases of small and large K, as well as for the hydrogen-like states. The reduced expansion over the basis of the states related to the ground Landau level $N = 0$ yields a good approximation for atomic energies, sizes and oscillator strengths of those radiative transitions which remain allowed at $K = 0$, although the basis functions with $N > 0$ should be included for other transitions. Wavefunctions, energies and radiative transitions in the discrete spectrum have been studied using the suggested approach.

Atoms with large K acquire large dipole moments. The electron density becomes shifted aside from the proton, although its shape remains close to cylindrical at all K, and the shifted adiabatic approximation gives a qualitatively correct impression of it. The energy spectrum is divided into different m-bands. The states with $m \neq 0$ become metastable at large K, while the band $m = 0$ includes the infinite number of really bound states at arbitrary K. The mean velocity of the transverse motion is proportional to K for small K, and it is inversely proportional to K^2 for large K. For each state, the velocity cannot exceed some maximum value.

The atomic energies, sizes and wavefunctions, obtained in this paper, are used elsewhere for computation of photoionization cross sections of the moving hydrogen atom (Bezchastnov and Potekhin 1993), and for calculations of ionization equilibrium of hydrogenic plasma in neutron star atmospheres (Pavlov *et al* 1993).

The oscillator strengths of the bound–bound radiative transitions undergo radical changes when the atom moves across the field. Some of them vary by several orders of magnitude. Moreover, since the z-projection of the angular momentum of the moving atom does not conserve formerly forbidden dipole transitions with $m_i - m_f \neq \alpha$ become allowed. Thus, the motion breaks some dipole selection rules and causes drastic changes in transition rates, confirming the predictions of Pavlov and Mészáros (1993).

Acknowledgments

I am pleased to acknowledge useful discussions with V G Bezchastnov, Y A Shibanov, D G Yakovlev, and V E Zavlin. I am especially grateful to George G Pavlov, who initiated this work and gave priceless advice during its realization. I express my gratitude to C J Pethick for the hospitality during my stay at Nordita. This work was supported through ESO C&EE Grant A-01-068.

Appendix. Effective potentials

The effective potentials in (18) consist of two terms. The constant term $\langle N''m''|H_K|N'm'\rangle$, which admixes neighbouring states $N'' = N' \pm 1$, $m'' = m' \pm 1$, is easily calculated with the help of well known expressions for the effect of operators $\pi_{\pm 1}$ and $r_{\pm 1}$ on the basis states $|Nm\rangle$ (Hasegawa and Howard 1961). The result is

$$\begin{aligned}\langle N'm'|H_K|Nm\rangle = {} & (K')^2/(2M)\delta_{N'N}\delta_{m'm} \\ & + (\mathrm{i}\hbar/a_\mathrm{M})\Big[\Big(w_{\mathrm{e},+1}\sqrt{N}\ \delta_{N',N-1} + w_{\mathrm{p},+1}\sqrt{N-m+1}\delta_{N'N}\Big)\delta_{m',m-1} \\ & - \Big(w_{\mathrm{e},-1}\sqrt{N+1}\delta_{N',N+1} + w_{\mathrm{p},-1}\sqrt{N-m}\delta_{N'N}\Big)\delta_{m',m+1}\Big] \end{aligned} \tag{A1}$$

where

$$\begin{aligned} \boldsymbol{w}_\mathrm{e} &= \boldsymbol{K}/M + e/(2m_\mathrm{e}c)\boldsymbol{B} \times (\boldsymbol{r}_\mathrm{B} - \boldsymbol{r}_\mathrm{A}) \\ \boldsymbol{w}_\mathrm{p} &= \boldsymbol{K}/M + e/(2m_\mathrm{p}c)\boldsymbol{B} \times (\boldsymbol{r}_\mathrm{B} + \boldsymbol{r}_\mathrm{A}). \end{aligned} \tag{A2}$$

In the particular case, when $r_{\mathrm{B}} = \eta r_{\mathrm{C}}$, one has $w_{\mathrm{e},\pm1} = w_{\mathrm{p},\pm1} = \pm \mathrm{i} K(1-\eta)/(M\sqrt{2})$, and the effective potential (A1) becomes real.

Let us turn to the effective Coulomb potential (19), assuming that r_{B} is directed along r_{C} (the general case of an arbitrary direction is easily recovered by a change of variables). With the aid of equation (13) we have

$$V_{Nm,N'm'}(z) = -\frac{e^2}{a_{\mathrm{M}}\sqrt{2}} v_{Nm,N'm'}\left(\frac{r_{\mathrm{B}}}{a_{\mathrm{M}}\sqrt{2}}, \frac{z}{a_{\mathrm{M}}\sqrt{2}}\right) \tag{A3}$$

where

$$v_{Nm,N'm'}(\rho,\zeta) = \int_0^{2\pi} \frac{\mathrm{d}\varphi}{2\pi} \mathrm{e}^{\mathrm{i}(m'-m)\varphi} \int_0^\infty \mathrm{d}\xi\, I_{N-m,N}(\xi) I_{N'-m',N'}(\xi) \times \left(\zeta^2 + \rho^2 + \xi - 2\rho\sqrt{\xi}\cos\varphi\right)^{-1/2} \tag{A4}$$

does not depend on γ. Since $v_{Nm,N'm'} = v_{N'm',Nm}$, we may assume $m - m' = q \geqslant 0$ without loss of generality. Using the Gauss decomposition of the last multiplier in the integrand, one can transform (A4) into

$$v_{Nm,N'm'}(\rho,\zeta) = \frac{2}{\sqrt{\pi}} \int_0^\infty \mathrm{d}\xi \int_0^\infty \mathrm{d}x\, I_{N-m,N}(\xi) I_{N'-m'}(\xi) \times I_q(2x^2\rho\sqrt{\xi}) \exp[-x^2(\zeta^2 + \rho^2 + \xi)] \tag{A5}$$

where $I_q(y)$ is the modified Bessel function. A direct integration in (A5) is rather time-consuming. To simplify it, let us make use of the explicit form of the Laguerre functions,

$$(-1)^{N-n} I_{N-m,N}(\xi) = I_{n+|m|,n}(\xi) = \xi^{|m|/2} \mathrm{e}^{-\xi/2} \sum_{k=0}^{n} a_{kn|m|}(-\xi)^k \tag{A6}$$

where $n = N - (m + |m|)/2$ is the radial quantum number, and

$$a_{kns} = [(n+s)!n!]^{1/2} [k!(n-k)!(s+k)!]^{-1}. \tag{A7}$$

Therefore each potential $v_{Nm,N'm'}$ is equal to a finite sum of potentials related to the ground Landau level:

$$v_{Nm,N'm'}(\rho,\zeta) = \sum_{l=0}^{n+n'} (-1)^{N-n+N'-n'+l} \sum_{k+k'=l} a_{kn|m|} a_{k'n'|m'|} \sqrt{s!s'!}\, v_{ss'}(\rho,\zeta) \tag{A8}$$

where $s = (|m| - m + |m'| + m')/2 + l$, $s' = (|m| + m + |m'| - m')/2 + l$, and $v_{ss'}(\rho,\zeta) \equiv v_{0,-s,0,-s'}(\rho,\zeta)$. The latter potential can be further simplified with the aid of the relation (Gradstein and Rydzhik 1965)

$$\int_0^\infty \mathrm{e}^{-X\xi} \xi^{s+q/2} I_q\left(2x^2\rho\sqrt{\xi}\right) \mathrm{d}\xi = s!X^{-(q+1)}(x^2\rho)^q \mathrm{e}^{x^4\rho^2/X} L_s^q(-x^4\rho^2/X) \tag{A9}$$

where $L_s^q(y)$ is an adjoint Laguerre polynomial. Substituting (A9) with $X = 1 + x^2$ into (A5), after simple transformations one obtains

$$v_{s,s+q}(\rho,\zeta) = \frac{\rho^q}{\sqrt{\pi}} \sum_{k=0}^{s} a_{ksq}\rho^{2k} \int_0^1 \exp[-\zeta^2 t/(1-t) - \rho^2 t] t^{q+2k-1/2} (1-t)^{s-k-1/2}\, \mathrm{d}t. \tag{A10}$$

This expression is feasible for numerical treatment using Gauss–Chebyshev quadratures (Abramowitz and Stegun 1972).

Finally let us consider the asymptotic behaviour of the potentials. It follows from (A5) that $v_{Nm,N'm'}(\rho,\zeta) \sim \rho^q$ at $\rho \to 0$. In particular, from (A10) one finds

$$v_{s,s+q}(\rho,0) = \frac{\Gamma(m+\frac{1}{2})\Gamma(s+\frac{1}{2})}{\sqrt{\pi}\, s!(s+q)!\, q!}\rho^q\left(1+\frac{2q+1}{2q+2}\frac{\rho^2}{2s-1}+\mathrm{O}(\rho^4)\right). \tag{A11}$$

In order to derive asymptotics of the effective potentials in the case $\zeta^2 \gg 1$ and $\zeta^2 \gg \rho^2$, the generating function (Kaminker and Yakovlev 1981) is convenient:

$$f_s(t) = \frac{\xi^{s/2}}{(1-t)^{s+1}}\exp\left[-\frac{\xi}{2}\frac{1+t}{1-t}\right] = \sum_{n=0}^{\infty}\sqrt{\frac{(n+s)!}{n!}}\, I_{n+s,n}(\xi)t^n. \tag{A12}$$

Substituting $f_{|m|}(t)$ and $f_{|m'|}(t')$ into (A5) instead of the Laguerre functions, integrating over ξ with the aid of (A9), where $X = 1+x^2+t/(1-t)+t'/(1-t')$, expanding the result in the power series over t and t', and taking into account the first relation (A6), one can express $v_{Nm,N'm'}(\rho,\zeta)$ as a finite sum of one-dimensional quadratures of the type of (A10) with some combinatorial coefficients. Equation (A10) presents the particular case $N = N' = 0$. Another particular case, corresponding to $\rho = 0$, has been presented by Friedrich and Chu (1983). If ρ is finite, only one of the terms of the sum survives at $\zeta \to \infty$, yielding the asymptotics

$$v_{Nm,N'm'}(\rho,\zeta) \sim \frac{C}{\sqrt{\pi}}\Gamma\left(r+\frac{1}{2}\right)\frac{\rho^q}{\zeta^{2r+1}} \tag{A13}$$

where

$$\begin{aligned}
&r = N - N' + q \qquad C = C_0[(N'-N)!q!]^{-1} \qquad \text{if } N \leqslant N' \\
&r = q \qquad C = C_0(-1)^{N-N'}N![N'!(N-N')!(N'-N+q)!]^{-1} \\
&\qquad\qquad \text{if } N-q \leqslant N' \leqslant N \\
&r = N - N' \qquad C = C_0^{-1}(-1)^q[(N-N'-q)!q!]^{-1} \qquad \text{if } N'+q \leqslant N
\end{aligned} \tag{A14}$$

and $C_0 = [n'!(n'+|m'|)!]^{1/2}[n!(n+|m|)!]^{-1/2}$.

In the case when ρ tends to infinity along with ζ, so that $\zeta/\rho =$ constant, the potentials decrease as $(\zeta^2+\rho^2)^{-(r+1/2)}$ with the same power indices r as in (A14), but with coefficients depending on the ratio ζ/ρ.

References

Abramowitz M and Stegun I A (eds) 1972 *Handbook of Mathematical Functions* (New York: Dover)
Avron J E, Herbst I W and Simon B 1978 *Ann. Phys., NY* **114** 431–51
Baye D and Vincke M 1990 *Phys. Rev.* A **42** 391–6
Baye D, Clerbaux N and Vincke M 1992 *Phys. Lett.* **166A** 135–9
Bezchastnov V G and Potekhin A Y 1993 *J. Phys. B: At. Mol. Opt. Phys.* submitted
Burkova L A, Dzyaloshinsky I E, Drukarev G P and Monozon B S 1976 *Sov. Phys.–JETP* **44** 276–8
Fletcher C A J 1988 *Computational Techniques for Fluid Dynamics 1* (Berlin: Springer)
Forster H, Strupat W, Rösner W, Wunner G, Ruder H and Herold H 1984 *J. Phys. B: At. Mol. Phys.* **17** 1301–19

Friedrich H 1982 *Phys. Rev.* A **26** 1827–38
Friedrich H and Chu M 1983 *Phys. Rev.* A **28** 1423–8
Froese Fischer C 1977 *The Hartree–Fock Method for Atoms: A Numerical Approach* (New York: Wiley)
Garstang R H 1977 *Rep. Prog. Phys.* 40 105–54
Gorkov L P and Dzyaloshinsky I E 1968 *Sov. Phys.–JETP* **26** 449–58
Gradstein I S and Rydzhik I M 1965 *Tables of Integrals, Series, and Products* 4th edn (New York: Academic)
Haines L K and Roberts D H 1969 *Am. J. Phys.* **37** 1145–54
Hasegawa H and Howard R E 1961 *J. Phys. Chem. Solids* **21** 179–98
Herold H, Ruder H and Wunner G 1981 *J. Phys. B: At. Mol. Phys.* **14** 751–64
Ipatova I P, Maslov A Y and Subashiev A V 1984 *Sov. Phys.–JETP* **60** 1037–9
Johnson B R, Hirschfelder J O and Yang K-H 1983 *Rev. Mod. Phys.* **55** 109–53
Johnson M H and Lippmann B A 1949 *Phys. Rev.* **76** 828–32
Kaminker A D and Yakovlev D G 1981 *Teor. Matem. Fiz.* **49** 241–53
Landau L D and Lifshitz E M 1976 *Quantum Mechanics* (Oxford: Pergamon)
Parlett B N 1980 *The Symmetric Eigenvalue Problem* (Englewood Cliffs, NJ: Prentice-Hall)
Pavlov G G and Mészáros P 1993 *Astrophys. J.* **416** 752–61
Pavlov G G, Potekhin A Y, Shibanov Y A and Zavlin V E 1993 *NATO ASI Lives of Neutron Stars (Kemer, Turkey, 1993)*
Pavlov G G, Shibanov Y A, Zavlin V E and Meyer R D 1994 *Lives of Neutron Stars* ed J van Paradijs and A Alpar (Dordrecht: Kluwer)
Potekhin A Y and Pavlov G G 1993 *Astrophys. J.* **407** 330–41
Rösner W, Wunner G, Herold H and Ruder H 1984 *J. Phys. B: At. Mol. Phys.* **17** 29–52
Simola J and Virtamo J 1978 *J. Phys. B: At. Mol. Phys.* **11** 3309–22
Sokolov A A and Ternov I M 1968 *Synchrotron Radiation* (Berlin: Academic)
Vincke M and Baye D 1988 *J. Phys. B: At. Mol. Opt. Phys.* **21** 2407–24
Vincke M, Le Dourneuf M and Baye D 1992 *J. Phys. B: At. Mol. Opt. Phys.* **25** 2787–807
Wunner G and Ruder H 1982 *J. Physique Coll.* **43** 137–52
—— 1987 *Phys. Scr.* **36** 291–9
Xi J, Wu L, He X and Li B 1992 *Phys. Rev.* A **46** 5806–11